Applied Catalysis B: Environmental 86 (2009) 196–205

Contents lists available at ScienceDirect

Applied Catalysis B: Environmental

journal homepage: www.elsevier.com/locate/apcatb

Influence of reaction products of K-getter fuel additives on commercial vanadia-based SCR catalysts
Part I. Potassium phosphate

Francesco Castellino [a], Anker Degn Jensen [a,*], Jan Erik Johnsson [a], Rasmus Fehrmann [b]

[a] Department of Chemical and Biochemical Engineering, Technical University of Denmark, DK-2800 Kgs. Lyngby, Denmark
[b] Centre for Sustainable and Green Chemistry, Department of Chemistry, Technical University of Denmark, Building 207, DK-2800 Kgs. Lyngby, Denmark

ARTICLE INFO

Article history:
Available online 14 November 2008

Keywords:
$DeNO_x$ SCR catalysts
Catalyst deactivation
Vanadia
Biomass
Potassium poisoning
Polyphosphoric acids

ABSTRACT

Commercial vanadia-based full-length monoliths have been exposed to aerosols formed by injection of K_3PO_4 (dissolved in water) in a hot flue gas ($T > 850$ °C) from a natural gas burner. Such aerosols may form when burning fuels with high K- and P-content, or when P-compounds are mixed with biomass as a K-getter additive. The formed aerosols have been characterized by using both a SMPS system and a low pressure cascade impactor, showing a dual-mode volume-based size distribution with a first peak at around 30 nm and a second one at diameters >1 μm. The different peaks have been associated with different species. In particular, the particles related to the 30 nm peak are associated to condensed phosphates, whereas the larger particles are associated to potassium phosphates. Two monoliths have been exposed during addition of 100 and 200 mg/Nm^3 K_3PO_4 for 720 and 189 h, respectively. Overall, deactivation rates up to 3%/day have been measured. The spent catalysts have been characterized by bulk chemical analysis, Hg-porosimetry and SEM-EDX. NH_3-chemisorption tests on the spent elements and activity tests on catalyst powders obtained by crushing the monoliths have also been carried out. The catalyst characterization has shown that poisoning by K is the main deactivation mechanism. The results show that binding K in K–P salts will not reduce the rate of catalyst deactivation.

1. Introduction

1.1. The K-getters fuel additives

The release of K-salts during biomass combustion is known to cause several problems to the boiler equipment downstream the boiler, thus limiting the application of this CO_2-neutral process [1]. Among these problems, the fast deposition rate on the super-heater exchangers of highly corrosive ashes is by far the most undesired. When biomass (e.g. straw and wood) is fired, the potassium in the fuel, which is released in the gas phase during combustion, forms aerosols of pure KCl and K_2SO_4 [2,3]. Potassium chloride has a relatively low melting point (i.e. 776 °C) and is therefore found in a melted-phase at the temperatures of the super-heater exchangers, making the ashes sticky. Ash deposition on the exchanger surfaces is therefore enhanced, causing a decrease in steam production efficiency. A periodical removal of these deposits, however, might not be sufficient in order to re-establish the original heat flux across the heat exchanger surfaces. In fact, since Cl is included in the formed deposits, these are very corrosive and a complete substitution of the tubing system might then be required in a shorter time than anticipated.

In order to limit these problems, Danish and Swedish power companies are currently evaluating the addition of different compounds to the biomass which are able to bind the potassium into particles with higher melting temperatures, while releasing the chlorine in the gas phase as HCl [4,5]. Sørensen et al. [6] developed a process where additives mainly constituted by P and Ca were mixed with the biomass in order to create the reaction conditions in the boiler at which the potassium gets captured in a phase consisting of $K_2O{\cdot}CaO{\cdot}P_2O_5$. As shown in Table 1, the compounds belonging to this system have melting points well above 1000 °C and will thereby not be found as melts at the super-heater section. Initial tests performed by feeding straw mixed with different additive compositions to an entrained flow reactor have shown a reduction of 74–98% of the level of Cl in the deposits when the molar ratios of P/(K + Na) and P/Ca in the resulting fuel mixture were in the ranges 1.9–3.2 and 0.8–0.9, respectively [7]. This seems

* Corresponding author. Tel.: +45 45 25 28 41; fax: +45 45 88 22 58.
E-mail address: aj@kt.dtu.dk (A.D. Jensen).

0926-3373/$ – see front matter © 2008 Elsevier B.V. All rights reserved.
doi:10.1016/j.apcatb.2008.11.009

Table 1
Possible products of biomass combustion and relative melting temperatures in the presence of K-getter fuel additives.

	T_m (°C)
$K_4P_2O_7$	1105
$K_2CaP_2O_7$	1143
K_3PO_4	1340
$KCaPO_4$	1560
$K_4Ca(PO_4)_2$	1645
$Ca_3(PO_4)_2$	1670

very promising from a deposition and corrosion point of view, but the addition process apparently requires an excess of both P and Ca with respect to the alkali fraction.

1.2. Additives influence on the SCR vanadia-based catalysts

Changes in fly ash composition due to the addition of P- and Ca-compounds might also have an effect on the equipment downstream the superheaters that must be adressed. Particularly sensitive to changes in both the fly ash content and composition is the selective catalytic reduction (SCR) process used for the abatement of the NO_x fraction of the flue gas [8]. This process relies on the ability of ammonia to selectively reduce the undesired NO_x present in the flue gas to molecular nitrogen according to the following global reactions:

$$4NH_3 + 4NO + O_2 \rightarrow 4N_2 + 6H_2O \quad (1.1)$$

$$2NO_2 + 4NH_3 + O_2 \rightarrow 3N_2 + 6H_2O \quad (1.2)$$

The most active and selective catalysts are mainly constituted by vanadium pentoxide (V_2O_5, total load varying between 1 and 5 wt% depending on the specific application), supported on a titania (TiO_2, anatase form) carrier. These are normally shaped into monoliths with parallel channels with hydraulic diameters up to 9 mm, which allows operation even in the presence of fly ash loads (>10 g/Nm^3) relevant for suspension firing before ESP with only low pressure drops over the reactor. A widely accepted mechanism of reaction for these catalysts at typical industrial operating conditions was proposed by Topsøe et al. [9,10]. This involves adsorption of NH_3 on Brønsted acid sites, activation of adsorbed ammonia by V=O species and subsequently reaction with gaseous or weakly adsorbed NO. Deactivation of vanadia-based catalysts can be due to poisoning, fouling, surface masking, pore blocking and sintering according to the particular application. In most of these cases, however, the fly ash plays an important role since it may act both as physical deactivating agent, and as a carrier for different chemical deactivating species. For instance K, which according to different studies is a very strong poison for the vanadia-based SCR catalysts [3,11–17], is present as solid particles at the SCR reactor inlet. Therefore the observed rate of deactivation is directly related to the fluid dynamics controlling the rate of particle deposition. However, important as well is the rate of particle/poison penetration into the catalyst walls, and this is more likely related to the way the K-fraction is bound to the particle itself. For instance, up to 1%/day deactivation has been measured both at a biomass-fired combined heat and power plant [3] and in a pilot plant [17] where K was present as aerosols of pure KCl and K_2SO_4. Contrary, accordingly to coal firing experience, when K is mainly bound to non-soluble silica-aluminates, the deactivation proceeds at much slower rates. In order to explain the influence of the particle composition on the different deactivation rates experienced, Zheng et al. [3] suggested that this is related to the K-mobility at the SCR temperatures. The reason for the good mobility of KCl and K_2SO_4 was found in the Hüttig and Tamman temperatures of these compounds. These two temperatures are normally used to estimate the temperatures at which sintering starts [18] and are calculated with the following empirical expressions:

$$T_{Hüttig} = 0.3T_{melting}$$

$$T_{Tamman} = 0.5T_{melting}$$

When the Hüttig temperature is reached, atoms at vacancies start being mobile. When the Tamman temperature is eventually reached, the atoms in the bulk start showing mobility. According to their Hüttig and Tamman temperatures, the atoms forming the KCl and K_2SO_4 deposits may then be expected to be mobile at the SCR temperatures, and therefore react with the catalyst surface and further diffuse on it.

The discussion above indicates that binding K to ashes with higher melting temperatures by the addition process may reduce the rate of deactivation by decreasing the poison penetration in the catalyst walls. On the other hand, the increased P- and Ca-levels induced by the additive process could to some extent counterbalance this positive effect. P and Ca are known to be deactivating species for the vanadia-based SCR catalysts [11,12,19–22]. The excess levels of P with respect to the alkali fraction in the resulting fuel mixture required by the addition process might lead to an undesired formation of polyphosphoric acids. In a previous investigation [22] the formation and deactivating mechanisms of polyphosphoric acids have been reported. H_3PO_4 was found to form aerosols of viscous liquid polyphosphoric acids with diameters <0.1 μm due to homogeneous nucleation occurring at temperatures <500 °C. These results were in agreement with the higher P-concentrations found in the submicron particles when coal was co-fired with P-rich secondary fuels at full-scale [23], or simply mixed with P-compounds and burned in an electrically heated plug flow reactor [24]. The polyphosphoric acid particles were characterized by very fast deposition rates due to both the high particle number and their high diffusivity due to their small size, and they caused a fast deactivation of the catalyst by both physical and chemical deactivation [22]. In particular, the chemical deactivation was related to the stabilization of V(4+) species formed as intermediate during the SCR reaction by the polyphosphoric acids. However, no other species (apart from O_2, CO_2, H_2O and N_2) were present in the flue gas during the tests, leaving the question about the formation of polyphosphoric acids in a *non-clean* system still open.

1.3. Objectives

This work is part of a project, which aims at evaluating the effects of the addition of Ca-, P-based K-getter species on the vanadia-based SCR catalysts. This paper focuses on the potassium phosphate system, since in this system some of the potential reaction products of the K-getter fuel additives are found. The results of the investigations carried out by exposing full-length commercial SCR monoliths to a flue gas doped with K_3PO_4 in a pilot-scale SCR setup for up to 700 h are reported. The second part of the work will focus on the simultaneous addition of KCl, $Ca(OH)_2$, H_3PO_4 and H_2SO_4 in the flue gas, to simulate a more complete full-scale addition process.

Apart from estimating the potential effect of the addition process on the SCR catalysts, the tests shown in this paper offer the possibility: (i) to provide further input to the mechanism of K-deactivation by aerosols; (ii) to determine the possible formation of polyphosphoric acids and thereby provide additional information about the P-release during combustion.

2. Experimental

2.1. Catalysts

Commercial corrugated-type monoliths obtained from Haldor Topsøe A/S were used in this study. The catalysts were based on V_2O_5 (up to 5 wt%) and tungsten oxide (WO_3, up to 9 wt%) dispersed on a fiber reinforced TiO_2 carrier. The monoliths had a size of 75 mm × 75 mm × 500 mm. The hydraulic diameter of the channels was 6.44 mm and the wall thickness was 1.0 mm. Pieces of both fresh and spent monoliths have been cut from both the inlet and the outlet in order to study their local properties under well defined reaction conditions in a laboratory fixed bed reactor. In order to run activity tests on powdered samples, they have been gently crushed in a mortar and the particle fraction in the range 105–125 μm has been collected by sieving.

2.2. SCR pilot plant

The SCR pilot plant setup used for this investigation is the same as described in [22]. Its main parts are a natural gas burner for flue gas production, a lance for injecting liquid solutions, a square duct hosting a full-length commercial monolith and a NH_3 supply system. NH_3 is injected both in the burner to produce the desired NO concentration at the reactor inlet, and in the flue gas duct leading to the reactor for the NO reduction. A soot blowing system running with compressed air is installed at the SCR reactor inlet to keep the monolith channels open.

2.3. K_3PO_4 addition

The addition of K_3PO_4 to the flue gas was performed by spraying water solutions through a two-fluid nozzle. The solutions were prepared by dissolving K_3PO_4 (reagent grade ≥98%, Sigma®) in distilled water. Two catalyst elements have been exposed to 100 and 200 mg/Nm^3 K_3PO_4. In this work they will be identified by the labels "KP100" and "KP200", respectively. The letters "T" and "B" added at the end of the labels will indicate a sample cut respectively from the top (first 10 cm) and the bottom (last 10 cm) of the element. In all tests, the salt concentration in the solutions was fixed at 21 g/L and the solution feed rate was then varied in order to get the desired concentration in the flue gas (i.e. 0.25 and 0.5 L/h to get 100 and 200 mg/Nm^3, respectively).

2.4. Aerosol measurements

2.4.1. Scanning Mobility Particle Sizer

A Scanning Mobility Particle Sizer (SMPS, TSI Inc.), which included an Electrostatic Classifier (Model 3080) and a Condensation Particle Counter (Model 3775) was used to measure the particle concentration and size distribution during the exposure to K_3PO_4. Particle sampling was carried out at the inlet of the SCR reactor by an ejector sampler running with dry, particle-free air. In this system the particle-containing flue gas was at the same time cooled and diluted thereby preventing: (i) water condensation; (ii) particle coagulation in the sample line by effectively decreasing its rate by several orders of magnitude; (iii) overloading of both the impactor and the SMPS. The dilution ratio, required to know the real particle concentration in the flue gas, was obtained by measuring the CO_2 concentration both in the flue gas and in the diluted sample.

2.4.2. Low pressure cascade impactor

A 10-stage Berner-type low pressure cascade impactor (LPI) with an aerodynamic diameter range of 0.03–12.7 μm connected to a vacuum pump was used. The flow through the LPI was controlled by a critical orifice and was equal to 22.49 L/min at 25 °C and atmospheric pressure. The flue gas was sampled directly at the reactor inlet without any dilution. Therefore the sampling line and the LPI were heated to 90 °C in order to avoid any water condensation. Deposited particles were collected on aluminum foils coated with a thin film of Apiezon H grease. The grease served to limit bouncing of the particles and was added using a dilute toluene solution of the grease. The toluene was evaporated from the foils by drying these in an oven at 140 °C for 2 h. The sampling time was equal to 60 min, which allowed a suitable collection of particle mass. The weight gains from the deposited particles on each foil were determined by a Sartorius M5D-000V001 microbalance. The foils were finally analyzed by electron dispersive X-ray analysis for chemical composition.

2.5. Activity measurements

The rate of the SCR reaction at typical industrial reaction conditions has been assumed to follow an Eley-Rideal mechanism of reaction with NH_3 adsorbed on the catalyst surface and NO reacting from the gas phase. The following expression for the rate of reaction, r_{NO}, can then be derived:

$$-r_{NO}\left[\frac{\text{mol}}{m_{cat}^3 s}\right] = k c_{NO} \frac{K_{NH_3} c_{NH_3}}{1 + K_{NH_3} c_{NH_3}} \tag{1.3}$$

where k [1/s] is the rate constant, c_{NO} and c_{NH_3} [mol/m^3] are the concentrations of NO and NH_3, respectively, and K_{NH_3} [m^3/mol] is the adsorption constant for NH_3 on the catalyst surface. The fraction term on the right-hand side of Eq. (1.3) is the NH_3 coverage of the catalytic surface, θ_{NH_3}.

At the pilot plant, the activities of the catalysts were measured at 350 °C in the presence of about 500 ppmv NO, 600 ppmv NH_3, 10 vol% O_2, 6 vol% CO_2, and about 10 vol% H_2O. During activity measurements the flow through the SCR reactor was kept at 40 Nm^3/h. At this flow the gas velocity in the channels were about 6.5 m/s at 350 °C, similar to the velocities used at full scale applications. At this velocity, up to 50% external mass transfer limitations have been estimated.

Since ammonia in our measurements is added in excess with respect to NO (i.e. $NH_3/NO \approx 1.2$), the NH_3 coverage, θ_{NH_3}, can be assumed equal to 1 and the reaction rate can be regarded as pseudo-first order with respect to NO and zero order with respect to NH_3. Therefore, directly from the fractional NO conversion, X, it is possible to calculate an observed catalyst activity constant, k', that includes both the influence of external and internal mass transfer:

$$k'\left[\frac{ml}{gs}\right] = -\frac{F_{gas}}{m_{cat}} \ln(1 - X) \tag{1.4}$$

where F_{gas} is the gas flow rate (ml/s), m_{cat} is the weight of catalyst (g). The degree of deactivation can then be calculated as the ratio k/k_0 between the activity constant of the catalyst during exposure, k, and the one measured for the fresh element, k_0, right before starting the poison addition.

In the laboratory, powdered samples have been tested for activity in a packed bed quartz micro-reactor with a diameter equal to 10 mm. Around 0.07 g of powder has been used during activity measurement. This has been mixed with sand of the same particle size in order to have a particle bed of about 10 mm, thus ensuring the applicability of the here assumed integral reactor model. In all experiments, the total flow was equal to 2.8 NL/min and was constituted by 500 ppmv NO, 600 ppmv NH_3, 5 vol% O_2 and 1.4 vol% H_2O in N_2. Activity measurements have been performed in the temperature range 250–400 °C. The catalyst

activity has been calculated according to Eq. (1.4) and the deactivation as the ratio between the activity constant of the spent catalyst and the one measured for the fresh one. At 350 °C, the observed activity constant, *k'*, for the fresh catalyst powder was found only 10% less than the one calculated in the total absence of mass transfer limitations. The latter value was calculated by extrapolating to higher temperatures a fit to the Arrhenius plot obtained in the kinetic regime in the range 250–330 °C.

During all activity measurements, the NO concentration in the flue gas has been measured with a conventional UV analyzer (Rosemount NGA 2000). Due to the presence of water in the gas composition during all activity measurements, no N_2O formation is expected [25].

2.6. Ammonia chemisorption

NH_3-chemisorption is the first step of the reaction mechanism [9,10], and poisoning by K has been found to decrease the amount of chemisorbed NH_3. Therefore, NH_3-chemisorption tests have been periodically carried out at the pilot-scale setup during the K_3PO_4 addition. The measurements have been made at 350 °C and 40 Nm^3/h. Around 600 ppmv NH_3 have been added to the flue gas and flow through the SCR reactor for 30 min in order to saturate the catalyst sites. Previous investigations made with the same catalysts showed that this period of time is sufficient to saturate all the sites available for NH_3-chemisorption on a fresh element. During this saturation period, only the NO produced by the natural gas combustion was present (i.e. ≈80 ppmv). After this time, the NH_3 was shut off and right after, around 500 ppm NO were produced by adding a stream of NH_3 to the burner. The amount of chemisorbed NH_3 can then be calculated by integrating over time the amount of reduced NO, due to the equimolar reaction between the gaseous NO and the chemisorbed NH_3.

2.7. Catalyst characterization

Small pieces of catalyst were cut from the ends of both fresh and exposed monoliths and characterized without further treatment with respect to bulk chemical composition, mercury porosimetry and physical appearance by a Scanning Electron Microscope (SEM).

The chemical composition was obtained by ICP-OES at the laboratory of DONG Energy A/S. Prior to the measurements, the samples were cut to 1.5 × 1.7 cm^2 and dried at 105 °C for 2 h before analysis.

The total pore volume and the pore size distribution of the different catalyst samples were made by mercury intrusion in a Micromeritics Autopore II 9220 porosimeter. SEM-EDX analysis was performed at the Danish Technological Institute using a Zeiss Ultra55 and an Oxford ISIS with a Pentafet X-ray detector. In particular, for each sample the EDX analysis was performed on three different areas of about 200 × 200 μm^2 each. The numbers reported in this work are the averages of the different measurements. The standard deviations of the measurements have been found <0.5, 2 and 2.8 wt% for V, K and P, respectively.

3. Results

3.1. Aerosol measurements at the pilot-scale setup

3.1.1. SMPS measurements

Fig. 1 shows the number-based and volume-based particle size distributions measured during the addition of 100 mg/Nm^3 K_3PO_4. According to the number-based distribution, the aerosols were characterized by a peak at around 30 nm. However, when the volume-based distribution is plotted instead, a second peak at higher diameter appears. In particular, it can be seen in Fig. 1b that this second peak almost entirely extends outside the upper detection limit of the SMPS used. By assuming a density for these particles equal to the density of K_3PO_4 (i.e. 2.564 g/cm^3), the total mass measured by the SMPS would be equal to around 8% of the injected one. This low value indicates that a great part of the injected mass is present at the larger diameters not detectable by the SMPS. By fitting the data obtained with a lognormal distribution, the curve showed in Fig. 1b can be obtained. The fitting has been made by minimization of

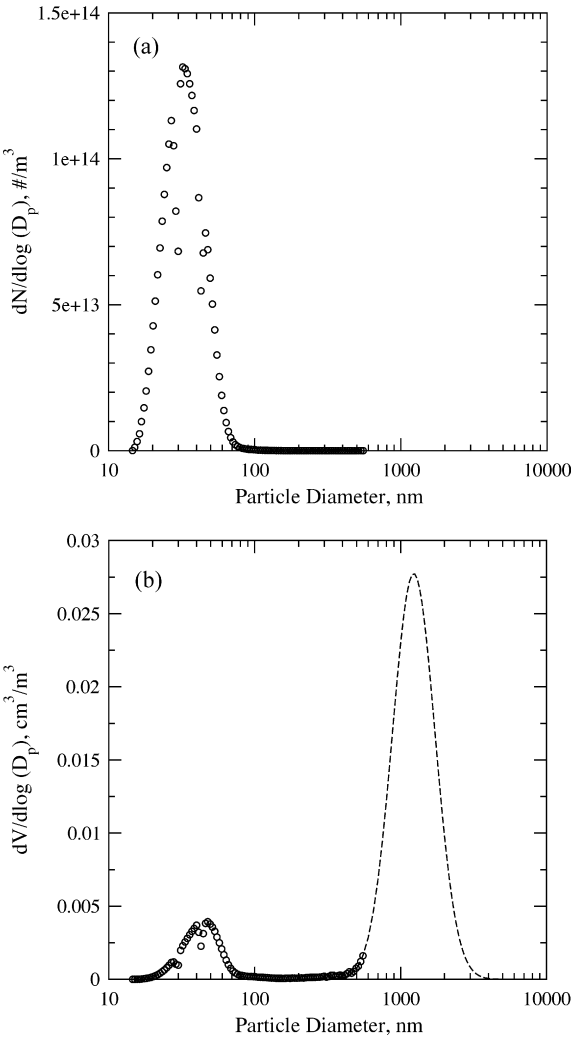

Fig. 1. Number-based (a) and volume-based (b) particle size distributions measured by SMPS at the reactor inlet during addition of 100 mg/Nm^3 K_3PO_4 at T = 350 °C. The dashed line represents a lognormal distribution derived by fitting the data points in the particle diameter range 300–550 nm.

$$\sum_{d_p}[\psi_{V,\mathrm{SMPS}}(d_p) - \psi_{V,logn}(d_p)]^2 \quad 300\,\mathrm{nm} \le d\,p \le 550\,\mathrm{nm} \qquad (1.5)$$

where $\psi_{V,\mathrm{SMPS}}$ is the volume distribution $dV/d(log\ dp)$ calculated from the SMPS measurement, $\psi_{V,logn}$ is the fitted distribution. The mean diameter of the lognormal distribution is equal to 1.25 μm. Overall, the total mass calculated is equal to around 40% of the injected K_3PO_4. Both the mean diameter and the total mass at the reactor inlet would then be comparable to previous tests carried out at this setup [17]. As will be discussed later, the presence of this dual-mode particle distribution is related to the presence of mainly two different species, whose formation has followed different mechanisms.

Table 2
K- and P-content measured on different impactor stages by EDX. The particles were collected during addition of 100 mg/Nm^3 K_3PO_4.

Impactor stage number	Particle Diameter (nm)	K (at.%)	P (at.%)	K/P (molar)
4	1488	47.31	13.8	3.48
5	754	51.22	15.39	3.33
6	382	48.66	16.65	2.92
7	193	48.49	14.82	3.27
8	98	47.49	14.8	3.21
9	49	44.08	14.71	3.00

3.1.2. Cascade low pressure impactor measurements

Tests with the LPI have been performed during both the KP100 and KP200 experiments. In all cases, the particles collected at the different stages were very liquescent and were therefore melting as soon as they were exposed to ambient air. The determination of the weight of the different foils was therefore problematic. Not only the foils were increasing their weight due to water adsorption. Some of them were at some point even loosing weight during their mass determination. This fact indicates that during exposure to ambient air at room temperature some gaseous species were released by the deposit. Due to these problems, the only partly useful indications obtained from the tests were those provided by the EDX analysis of the different foils reported in Table 2. Here, values of the K:P molar ratio in the range 3–3.5 were measured, which are slightly higher than the expected value of 3. Interestingly, the K:P values were increasing with the collected particle size (apart from the value measured on stage #6). These values may differ from the expected value of 3 simply because experimental uncertainity of the EDX measurements, but, recalling the particle size distribution measured by the SMPS, they may also indicate that part of the P was not collected on the lower impactor stages, probably because the remaining fraction was present in even smaller particles or in the gas phase.

3.2. Catalyst characterization

3.2.1. Bulk and surface chemical analysis

Table 3 reports the results of both the bulk and surface chemical analysis for the elements KP100 and KP200. The K-content in the bulk was varying in the range 0.8–2.5 wt%, whereas the P-content was varying in the range 0.4–0.8 wt%. Apart from the K-content in KP200, both the levels of K and P found in the bulk of the two elements were decreasing from the top to the bottom in agreement with both the higher particle concentration and the higher mass transfer due to the developing flow and higher level of turbulence at the top. About double levels of K were found on KP100 compared to KP200, whereas the levels of P were roughly the same. The calculated bulk K:P molar ratios were in the range 0.85–2.52 and therefore less than 3, which is the value introduced into the system by the K_3PO_4 molecule, indicating a different path for the accumulation of K and P in the catalyst walls.

Regarding the external surface composition measured by SEM-EDX shown in Table 3, very high concentrations of P have been found. In particular, the element KP200 reported P-concentrations up to 12.6 wt%. In the case of KP100, the P-content was ranging between 1.0 and 2.8 wt%. The cross sections of the samples KP100B and KP200T shown in Fig. 2 have also been analyzed by SEM-EDX in order to measure the distributions of K and P along the catalyst walls. The results of the EDX measurements are shown in Fig. 3a and c. As shown in the plots, both the K- and P-content decrease as a function of catalyst wall depth, indicating a diffusion limited process. Only in the case of KP100B, the K-content is almost constant around 0.7 wt% throughout the analyzed wall thickness. However, the major difference between the K- and P-distributions is that, in the case of K, the concentration in the walls always appears to level off at a finite K-level (i.e. 0.7 wt% in the cases shown in Fig. 3a), whereas the P-concentration decreases to zero.

Table 3
Bulk, surface and Hg-porosimetry analysis for the fresh and spent monoliths.

	Fresh	KP100T	KP100B	KP200T	KP200B
Total exposure time (h)		720	720	189[a]	189[a]
Bulk chemical analysis					
V (wt/wt%)	1.60	2.46	1.61	1.76	2.70
K (wt/wt%)	0.0	2.45	1.44	0.80	0.90
P (wt/wt%)	0.01	0.77	0.46	0.75	0.40
K/P (mol/mol)		2.52	2.46	0.85	1.79
K/V (mol/mol)		1.30	1.17	0.59	0.44
P/V (mol/mol)		0.31	0.47	0.70	0.24
Surface chemical analysis					
V (wt/wt%)	2.1	2.1	3.5	2.4	2.2
K (wt/wt%)	0.0	1.7	0.8	6.2	2.1
P (wt/wt%)	0.0	2.8	1.0	12.6	6.2
K/P (mol/mol)		0.5	0.7	0.4	0.3
K/V (mol/mol)	0.0	1.1	0.3	2.7	1.2
P/V (mol/mol)	0.0	2.2	0.5	7.1	4.5
Hg-porosimetry					
Total intrusion volume (ml/g)	0.71	0.71	0.67	0.67	0.64
Total pore area (m^2/g)	36.84	37.04	37.65	48.66	39.46
Catalyst bulk density (g/ml)	0.96	0.94	1.01	1.03	1.11
Porosity (%)	68.60	66.92	67.66	69.64	70.78

[a] This exposure time does not include the lance blocking.

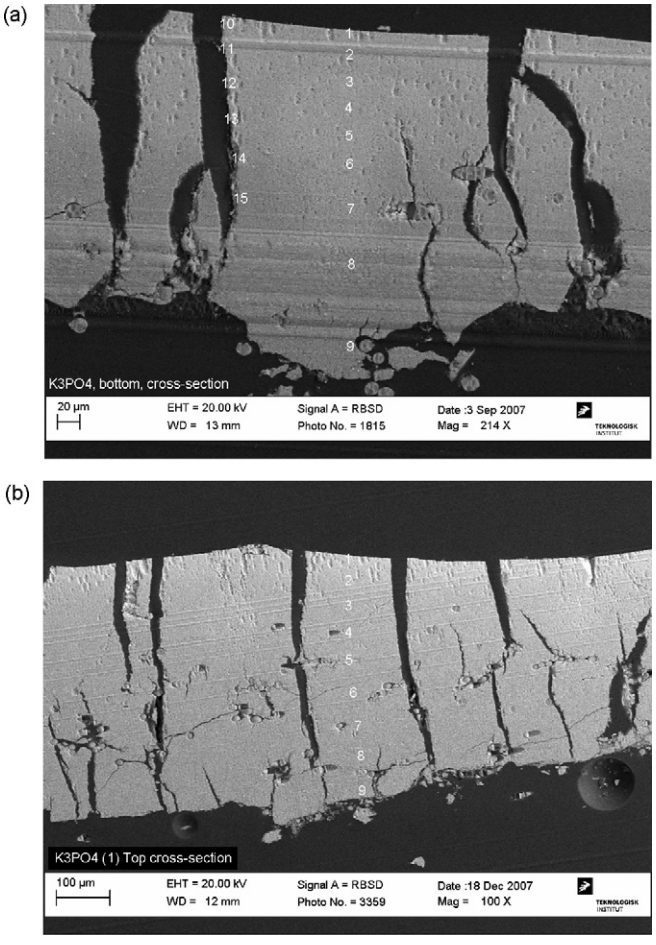

Fig. 2. SEM picture of the cross section of KP100B (a) and KP200T (b).

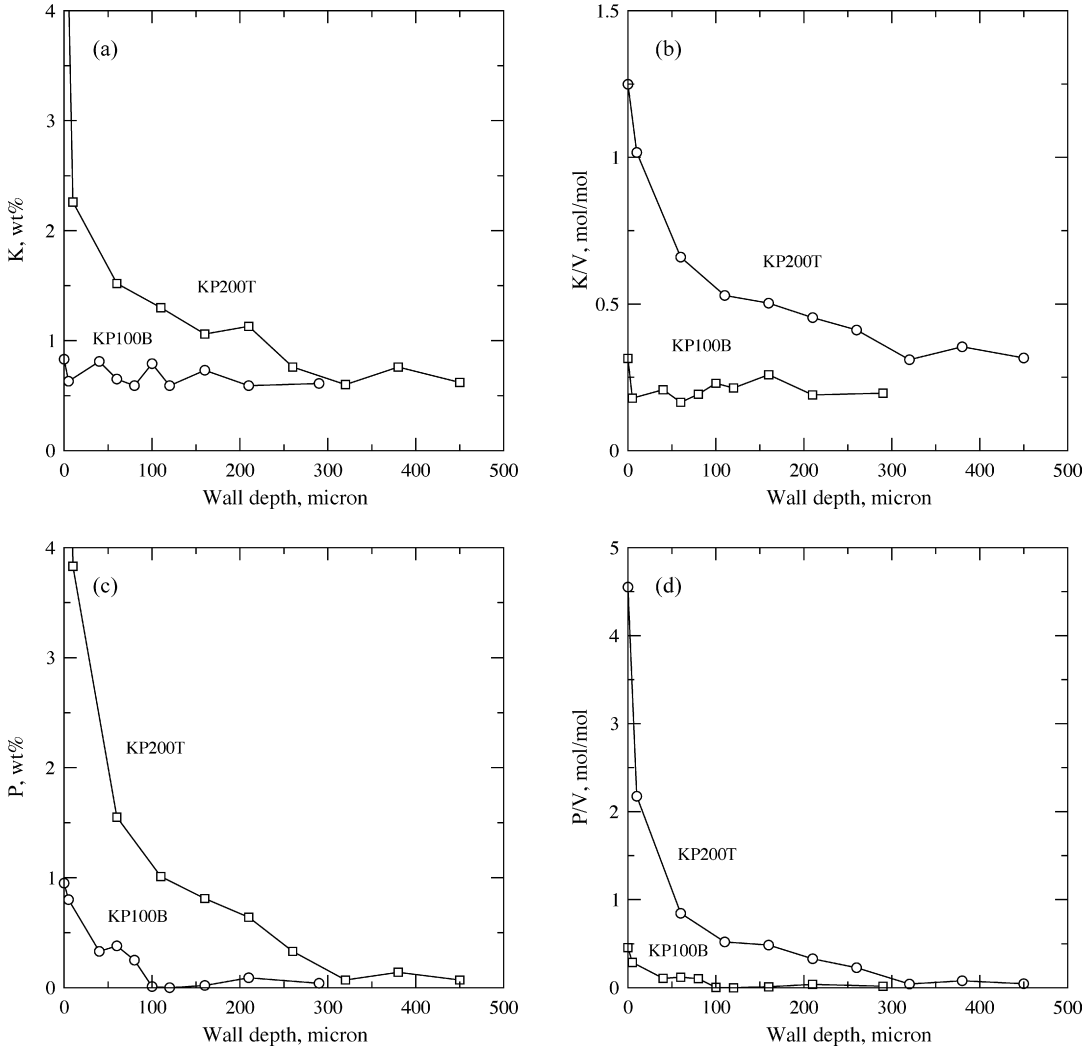

Fig. 3. K- and P-content and K:V and P:V molar ratios along the KP100B and KP200T walls as measured by SEM-EDX.

From these profiles, it appears that K tends to penetrate and remain in the catalyst wall, whereas P either is characterized by a slower mobility compared to K, or its penetration is counterbalanced by simultaneous evaporation of P as it was shown in our previous study [22]. As expected, in the presence of higher total K_3PO_4 concentrations in the flue gas, both K and P tend to accumulate on the outer catalyst surface.

Finally, Fig. 3b and d shows the calculated values for the K:V and P:V molar ratios, which can be used to estimate the local activities of the catalyst wall. According to values found in the literature [11,12], for K:V molar ratios equal to 0.2, up to 70% deactivation in the absence of mass transfer limitations can be expected.

3.2.2. Hg-porosimetry

The pore size distribution of the fresh and spent catalysts has been measured in order to clarify the presence of physical deactivation by pore blocking due to deposition of K–P particles. Fig. 4 reports the results of this investigation. The PSD of the fresh catalyst is clearly a dual-mode distribution, with the first peak found in the region 0.6–300 μm at 90 μm, and the second one in the region 0.003–0.6 μm at 0.03 μm. This dual-mode distribution is basically conserved in all spent catalyst samples. No major differences indicating pore blocking are found between the fresh and spent samples apart from the region 0.6–8 μm. Here, the spent samples consistently show almost no pores, whereas the fresh one has a considerable amount of them. In particular, the porosity for the fresh sample in this diameter range has been calculated to be equal to 6.93%. This value dropped to 1.35 and 0.89% for KP100T and KP100B, respectively, and 1.32 and 1.19% for KP200T and KP200B, respectively. However, no major difference in the total intrusion volume of the spent catalysts compared to the fresh sample was found (Table 3). This fact may indicate that the sample outer wall layer, which is the first that gets in contact with Hg during the measurement, had no pores in that range due to deposit build-up and/or pore blocking, but kept the original structure of the inner wall.

3.3. Deactivation at the pilot-scale setup

3.3.1. Activity measurements

The results of the activity measurements carried out during exposure to 100 and 200 mg/Nm^3 K_3PO_4 are shown in Fig. 5. Overall the measured deactivation rate was increasing according to the K_3PO_4 concentrations in the flue gas. In both cases, the deactivation was very fast at the beginning of the exposure: The two elements lost respectively 26 and 31% of their original activity during the first 72 h. After this initial period, the deactivation proceeded at slower but still appreciable rates.

The addition of 100 mg/Nm^3 was carried out for 720 h. After this period of time, the element was exposed to *clean* flue gas for

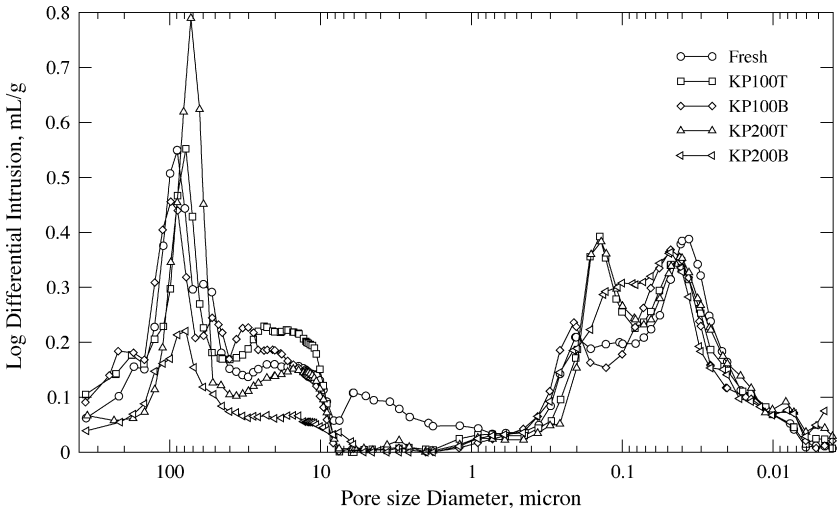

Fig. 4. Pore size distribution for fresh and spent samples measured by Hg-porosimetry.

additional 288 h, before it was taken out and characterized. The relative activity at the end of the addition time was 62%, corresponding to an overall deactivation rate of about 1.3%/day. During the subsequent exposure to the *clean* flue gas, the element regained 9% of relative activity. In particular, 7% was regained after the first 24 h after the addition was shut off. During these 24 h, the pressure drop over the monolith decreased by 11% indicating some cleaning of the channels due to soot blowing, which was continued after the addition stopped.

The addition of 200 mg/Nm^3 was carried out for only 280 h and was more problematic than the previous test. Due to the higher K_3PO_4 load, the two-fluid nozzle used for atomizing the water solution tended to clog due to salt deposition. In particular, the compressed air line right at the meeting point with the liquid solution was the one that had the higher tendency in getting clogged. When this happened, the solution was not correctly atomized and was eventually introduced as a liquid jet. The jet was then simply hitting the hot pipe walls right after the lance and forming massive deposits of salt. Clogging of the nozzle mainly happened two times: After 89 and 284 h from the addition start. In both cases, the activity measurement performed after the clogging showed an increased relative activity of the element compared to the previous test. These facts are in agreement with the result obtained with the element KP100, when this latter was exposed to a *clean* flue gas as discussed before. Overall, at the end of the experiment, the element KP200 had lost 22% of its original activity. However, the minimum relative activity was measured after 284 h during the last activity measurement before the nozzle clogged for the second time. Here the relative activity was equal to 73%, corresponding to a deactivation rate equal to about 2.3%/day.

3.3.2. NH_3-chemisorption tests

Fig. 6 shows the results of NH_3-chemisorption tests made with the element KP100 and KP200 during the addition of K_3PO_4. Since the amount of reduced NO is assumed equal to the amount of NH_3 chemisorbed on the catalyst surface, a longer time for the NO measured at the outlet to equalize to the value measured at the inlet indicates that more NH_3 is chemisorbed on the catalyst. From Fig. 6 it can be seen that the fresh element was able to chemisorb a higher amount of NH_3, and that this was decreasing as a function of the exposure to K_3PO_4. In particular, after 408 h of exposure the

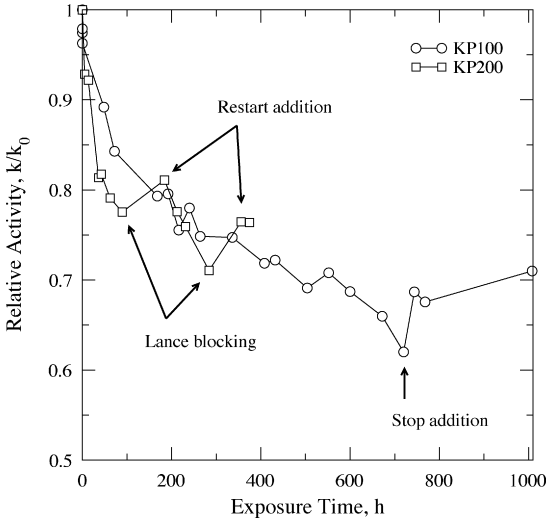

Fig. 5. Relative activity as a function of exposure time. Total flow: 40 Nm^3/h. Gas composition: NO = 500 ppmv, NH_3 = 600 ppmv, O_2 = 10 vol%, CO_2 = 6 vol%, and 10 vol% H_2O in N_2. T = 350 °C.

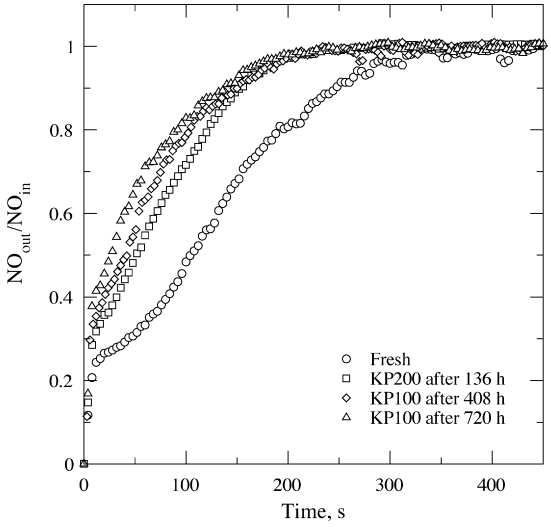

Fig. 6. NH_3-chemisorption test for the element exposed to 100 mg/Nm^3 K_3PO_4 at different times during the exposure. T = 350 °C.

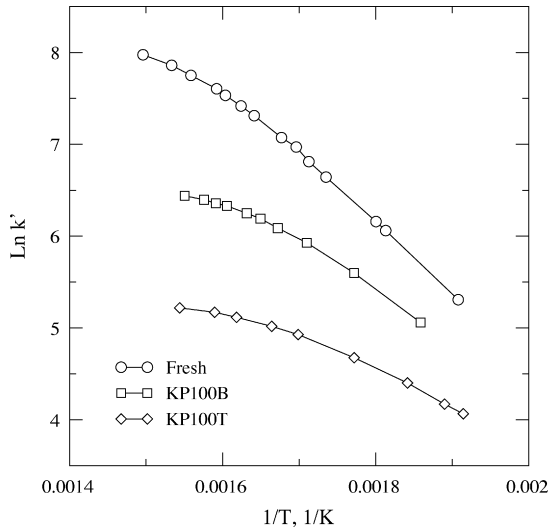

Fig. 7. Activity measurements on powdered samples. Total flow: 2.8 NL/min. NO = 521 ppmv; NH_3 = 622 ppmv; O_2 = 5.2%; H_2O = 1.47%; N_2 balance. Catalyst mass W = 0.072 g. Particle size: 105–125 μm.

amount of chemisorbed NH_3 on KP100 was about 54% of the fresh one. After 720 h, this further dropped to 47%. These results indicate that the deactivation was proceeding by deactivation of the sites for the NH_3-chemisorption.

3.4. Activity measurements in the laboratory

Fig. 7 shows an Arrhenius plot of the activities of powdered samples taken from the top and the bottom of the element KP100, together with a measurement made on a powdered fresh catalyst. The plot only reports the results in the temperature range 250–400 °C. In this range of temperatures, at the chosen experimental conditions, no external mass transfer limitations are present. Due to its very high activity, the fresh sample is subjected to some internal mass transfer limitations, as shown by the bending of the straight line at the higher temperatures in the Arrhenius plot (i.e. ≈ 10% at 350 °C). Due to the lower activity of the KP100T and KP100B samples, internal mass transport limitations are not responsible for the bending of the lines shown in the Arrhenius plot for these two doped samples. These may instead be the consequence of an increased activity in NH_3 oxidation at higher temperatures for the K-doped samples, as it was found in a previous work on K-poisoning [16].

As expected from the K- and P-content of the KP100 monolith, the top of the catalyst is more deactivated than the bottom. At 350 °C the relative activities for the top and the bottom of the element are equal to 9.1% and 30.0%, respectively.

4. Discussion

4.1. K- and P-accumulation and penetration mechanisms

The bulk chemical analysis of the catalyst composition has shown a K:P molar ratio less than the theoretical value of 3, varying in the range 0.85–2.5. The same ratio was always lower than 1 on the outer surface. Assuming a reaction between the catalyst surface and the K_3PO_4 particles leading to accumulation of K in the wall and release of H_3PO_4 in the gas phase, in a similar way as the release of HCl from KCl on the catalyst surface [3], the resulting K:P molar ratio should have then been found higher than 3. This fact is clearly in contrast with the results of the bulk chemical analysis and indicates that the deposited particles are not only constituted by K_3PO_4.

Further confirming this fact is the dual-mode particle size distribution measured by the SMPS. As discussed above, both particles with a volume-based mean diameter around 30 nm and particles with diameters exceeding the upper limiting range of the SMPS were present in the gas. Simply based on their size, the following can be assumed for these two classes of particles:

1. Low particle diameters and high number concentrations indicate particle formation due to homogeneous nucleation in the gas phase. In other words, the particles with mean diameters of 30 nm are constituted by species which can be found in the gas phase at relatively high temperatures. Contrarily, particles with diameters up 1 μm are more likely formed due to salt crystallization during water evaporation from the atomized aqueous solution according to their different solubilities.
2. The deposition rate of the smaller particles is higher due to the higher diffusion coefficients for these particles. In the presence of differences in the chemical composition as a function of particle size, the element characterizing the population with the higher number concentration and smaller particle diameters will accumulate faster on the catalyst surface.

In the absence of a detailed determination of the particle chemical composition due to the encountered experimental limitations, the scenario plotted in Fig. 8 is proposed.

1. *Condensate phosphates formation*. Potassium phosphate salts are reported to form condensate phosphates [26], here referred to as "KPO_x"

$$2K_3PO_4 \rightarrow K_4P_2O_7 + K_2O \quad (1.6)$$

$$K_4P_2O_7 + K_3PO_4 \rightarrow K_5P_3O_{10} + K_2O \quad (1.7)$$

From these reactions K_2O is formed. According to equilibrium calculations performed in this work by using the commercial software FactSage 5.2, the formed K_2O will be converted to KOH by reacting with the flue gas moisture. At lower temperatures K_2CO_3 will be formed by reaction with CO_2.

2. *KH_2PO_4 formation*. Crystallization of salts which are not the thermodynamic stable phases under the conditions of crystallization is reported to be rather common for the potassium orthophosphate system [26]. This means that the salts formed during the fast water evaporation from every single K_3PO_4 solution drop sprayed into the flue gas may differ from the initial K_3PO_4. Table 4 shows the known P–K salts and their solubility in water. In this, the solubility for KOH is also reported. As it can be seen, KH_2PO_4 is the salt with the lowest solubility. This indicates that this compound is the first that precipitates when water evaporates from a drop in the hot flue gas. The remaining K, which is not bound to the formed KH_2PO_4 will later precipitate as KOH

$$K_3PO_4 + 2H_2O \rightarrow KH_2PO_4 + 2KOH \quad (1.8)$$

Part of the P may also lead to some H_3PO_4. After water evaporation, the formed aerosols will be heated by the

Table 4
Solubility and melting temperature for different K-species.

	Solubility (g/100 g H_2O)	Melting temperature (°C)
K_3PO_4	106	1340
K_2HPO_4	168	dec. 465
KH_2PO_4	25	253
KOH	121	406
K_2CO_3	111	891

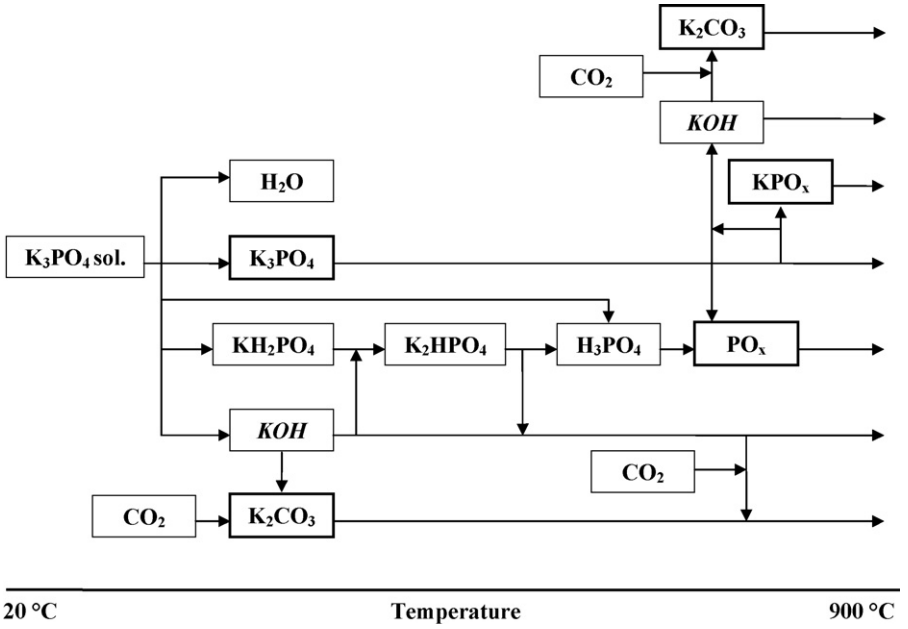

Fig. 8. Possible reactions during heating of K_3PO_4 solution droplets. The compounds in bold boxes are the ones most likely found at the SCR reactor inlet.

surrounding flue gas, and both the formed KH_2PO_4 and KOH are then converted to the more stable K_2HPO_4:

$$KH_2PO_4 + 2KOH \rightarrow K_2HPO_4 + KOH + H_2O \quad (1.9)$$

At temperatures higher than 465 °C the K_2HPO_4 will finally decompose. This decomposition may lead to formation of gaseous H_3PO_4. Moreover, the formed KOH will be converted to solid K_2CO_3 by reaction of KOH with CO_2:

$$K_2HPO_4 + 2H_2O \rightarrow H_3PO_4 + 2KOH \quad (1.10)$$

$$2KOH + CO_2 \rightarrow K_2CO_3 + H_2O \quad (1.11)$$

In both cases, the formation of H_3PO_4, KPO_x, K–P-salts with K:P molar ratios lower than 3 and some K_2CO_3, at the expenses of some of the original K_3PO_4 is foreseen. Among these species, H_3PO_4 can be regarded as responsible for the formation of the aerosols with mean diameter equal to 30 nm. Similar results have in fact been obtained during our previous investigation [22]. In this way, the high P-content on the outer catalyst surface measured by SEM-EDX would be explained, since it would be due to the higher deposition rates for these small particles compared to the bigger ones, where K is concentrated. Regarding the presence of K_2CO_3, this cannot be proved by the tests carried out in this work. However, the relatively high K:P molar ratios measured on the impactor stages may be considered as an indication of the presence of P-free K-particles. Moreover, it can be argued that the gas released by the deposits collected with the impactor was CO_2. Most of the compounds present in Fig. 8 are deliquescent, and therefore form a liquid solution when exposed to the ambient air, in agreement with the experience of the collected deposits. In this liquid solution then, release of CO_2 could be possible due to recombination of the species in the liquid phase, and could be favoured by the presence of acid compounds like the polyphosphoric acids.

The SEM-EDX of the catalyst wall cross sections indicate a faster net penetration for K compared to the one measured for P. Even though there still is an uncertainty about the real composition of the aerosols involved in the performed tests, and the presence of different species have been assumed, these different penetration rates are not likely associated to the presence of different species with different particle sizes and mobilities in the solid state. These are instead more likely associated with the different affinities between the elements K and P towards the acidic surface of the catalyst. It is here assumed that *solid-state acid–base reactions* are the major driving force responsible for reaction between the K-atoms from the particles and the catalyst surface. Since particles are deposited at the outer layers of the catalyst walls, a K-surface-gradient in the wall is first formed. This gradient is then responsible for the further penetration/distribution of the K-atoms by *surface diffusion*. On the other hand, P is included in acidic compounds. Consequently, acid–base reactions between the P-containing particles and the catalyst surface are not expected. The penetration of P is then mainly controlled by capillary forces applied on the viscous liquid phase the polyphosphoric acids are made of, and possibly K–P solid particle diffusion in the external layers of the catalyst walls. Furthermore, considering that the PO_x are hydrolyzed by the flue gas moisture at the reactor temperature releasing gaseous H_3PO_4 [22], the P-concentration in the wall will approach zero as observed. This would in fact be the result of combined particle deposition and P-evaporation. The P which is included in K–P salts might also leave the particle as H_3PO_4 when the K reacts with the catalyst surface.

4.2. Deactivation mechanism

The exposure of the commercial monoliths used in this work to a flue gas containing aerosols of K- and P-species has rapidly lowered the activity of the tested elements. In the absence of particles, the deactivation did not continue any further. On the contrary, when the exposure was performed without any K_3PO_4 addition, some reactivation of the catalysts was observed (9%). These facts indicate that (i) the aerosols are necessary to get any deactivation; (ii) reversible physical deactivation by outer surface fouling is contributing to the measured deactivation. According to the K-content measured by SEM-EDX analysis and the activity measurements made on powders, an agreement with the poisoning data from the literature has been found. For instance, the SEM-EDX analysis for the sample KP100B showed a constant K:V value of 0.2 along the whole wall. For the same sample, the relative intrinsic activity measured on powder was equal to 30% at

300 °C (Fig. 7), in good agreement with previous studies of K-poisoning [11,12]. This fact and the results of the NH_3-chemisorption tests indicate that the deactivation measured is mainly due to poisoning by K via blocking of the active sites for NH_3-chemisorption as reported in previous works [3,11-15]. The influence of poisoning by polyphosphoric acid is in this work not significant due to: (i) the relative low levels of P found due to simultaneous hydrolysis of the deposited acids; (ii) their relative low poisoning strength compared to K; (iii) a possible lowering of the deactivation strength of the polyphosphates due to the presence of K.

Physical deactivation due to pore blocking or surface masking by particle deposition is not likely to be the main mechanism responsible for the deactivation measured, but it is clearly contributing to the overall deactivation as indicated by the partial reactivation obtained by exposing the spent monoliths to clean flue gas while soot blowing. In particular, the almost complete disappearance of the pores in the range 0.6–8 μm for all the spent catalysts, together with the small loss (i.e. 6%) of the total intrusion volume are indications of the formation of an outer fouling layer. With up to 12 wt% P found on the outer catalyst surface, and since the polyphosphoric acids are viscous liquids at the SCR temperature [22], it is believed that they are playing an important role in the formation of this fouling layer by gluing togheter the different deposited particles. In general, an efficient soot blowing system is required not only to keep the channels opened, but also to clean their external surface.

5. Conclusion

K_3PO_4 has been indicated as a potential product of combustion of biomass mixed with P- and Ca-based K-getter additives for reducing fouling and corrosion problems on superheater surfaces at power stations. In order to evaluate whether the formation of this compound might also have a positive effect on the vanadia-based SCR catalysts by limiting the fast rate of deactivation normally experienced with KCl or K_2SO_4, K_3PO_4 has been added in a hot flue gas at a SCR pilot-scale setup and the activity of two commercial vanadia-based monoliths has been followed as a function of exposure time.

During the performed tests, different K- and P-compounds have been formed from the originally injected K_3PO_4. A dual-mode volume-based particle distribution with peaks at around 30 nm and at diameters >1 μm has been measured at the SCR reactor inlet. The distribution of K and P in the different particles has thereby influenced the rate of deposition and accumulation of the species in the exposed catalysts. In order to explain the high P-concentrations and low K:P molar ratios found on the outer catalyst surface, the smaller particles have been associated with liquid phase phosphates (PO_x and KPO_x), whereas the larger ones have been associated to potassium phosphates formed during evaporation of water from the injected droplets.

Deactivation rates up to 3%/day have beeen measured. K has been found to penetrate the whole catalyst wall indicating that this is not strongly bound to the particles and relatively fast reacts with the catalyst surface and subsequently penetrates the catalyst wall by surface diffusion. The NH_3-chemisorption studies have shown that the deactivation has mainly proceeded via K-poisoning by blocking the sites for NH_3 adsorption. All these data recall the mechanism of deactivation previously reported during exposures to KCl and K_2SO_4 and therefore indicate that binding K to P by the addition process does not seem to be an advantageous solution with respect to the vanadia-based SCR catalysts.

Poisoning by polyphosphoric acids is not clearly seen in this investigation due to both the relatively low P-content in the catalyst and the low poisoning strenght compared to K. However, Hg-porosimetry has revealed the occurrence of fouling and pore mouth blocking at the outer catalyst surface. It is believed that the polyphosphoric acids play an important role in the formation of this layer by gluing together the deposited particles and should therefore be considered a fouling promoter.

Acknowledgments

This work is part of the CHEC (Combustion and Harmful Emission Control) Research Center funded a.o. by the Technical University of Denmark, the Danish Technical Research Council, the European Union, the Nordic Energy Research, Dong Energy A/S, Vattenfall A.B., F L Smidth A/S, and Public Service Obligation funds from Energinet.dk and the Danish Energy Research program. In particular, this work is supported by the PSO project "Deactivation of SCR Catalysts by Additives" (PSO Elkraft FU-4205). Supply of the catalyst samples by Haldor Topsøe A/S is gratefully acknowledged.

References

[1] L.L. Baxter, T.R. Miles, T.R. Miles Jr., B.M. Jenkins, T. Milne, D. Dayton, R.W. Bryers, L.L. Oden, Fuel Processing Technology 54 (1998) 4778.
[2] K.A. Christensen, H. Livbjerg, Aerosol Science and Technology 25 (1996) 185–199.
[3] Y. Zheng, A.D. Jensen, J.E. Johnsson, Applied Catalysis B: Environmental 60 (2005) 261–272.
[4] Å. Kling, C. Andersson, Å. Myringer, D. Eskilsson, S.G. Järås, Applied Catalysis B: Environmental 69 (2007) 240–251.
[5] L. Tobiasen, R. Skytte, L.S. Pedersen, S.T. Pedersen, M.A. Lindberg, Fuel Processing Technology 88 (2007) 1108–1117.
[6] L. Sørensen, J. Fjellerup, U. Henriksen, International Publication Number WO 01/05911 A2. (2001).
[7] P.A. Jensen, L.H. Sørensen, G. Hu, J.K. Holm, F. Frandsen, U.B. Henriksen. Technical University of Denmark (2005) KT-Report No. 0504.
[8] V.I. Parvulescu, P. Grange, B. Delmon, Catalysis Today 46 (1998) 233–316.
[9] N.-Y. Topsøe, H. Topsøe, J.A. Dumesic, Journal of Catalysis 151 (1995) 226–240.
[10] N.-Y. Topsøe, J.A. Dumesic, H. Topsøe, Journal of Catalysis 151 (1995) 241–252.
[11] J.P. Chen, M.A. Buzanowski, R.T. Yang, Journal of the Air and Waste Management Association 40 (1990) 1403–1409.
[12] J.P. Chen, R.T. Yang, Journal of Catalysis 125 (1990) 411–420.
[13] L. Lietti, P. Forzatti, G. Ramis, G. Busca, F. Bregani, Applied Catalysis B: Environmental 3 (1993) 13–35.
[14] H. Kamata, K. Takashi, C.U.I. Odenbrand, Journal of Molecular Catalysis A: Chemical 139 (1999) 189–198.
[15] R. Khodayari, C. Andersson, C.U.I. Odenbrand, L.H. Andersson, Proceeding of the Fifth European Conference on Industrial Furnace and Boilers, vol. II, 11–14 April 2000, Espinho, Porto, Portugal, 2000.
[16] Y. Zheng, A.D. Jensen, J.E. Johnsson, Industrial and Engineering Chemistry Research 43 (2004) 941–947.
[17] Y. Zheng, A.D. Jensen, J.E. Johnsson, Applied Catalysis B: Environmental 83 (2008) 186–194.
[18] J.A. Moulijn, A.E. van Diepen, F. Kapteijn, Applied Catalysis A: General 212 (2001) 3–16.
[19] J. Blanco, P. Avila, C. Barthelemy, A. Bahamonde, J.A. Odriozola, J.F. Garcia de la Banda, H. Heinemann, Applied Catalysis 55 (1989) 151–164.
[20] H. Kamata, K. Takahashi, C.U.I. Odenbrand, Catalysis Letters 53 (1998) 65–71.
[21] J. Beck, J. Brandenstein, S. Unterberger, K.R.G. Hein, Applied Catalysis B: Environmental 49 (2004) 15–25.
[22] F. Castellino, S.B. Rasmussen, A.D. Jensen, J.E. Johnsson, R. Fehrmann, Applied Catalysis B: Environmental 83 (2008) 110–122.
[23] J. Beck, R. Müller, J. Brandenstein, B. Matschenko, J. Matschke, S. Unterberger, K.R.G. Hein, Fuel 84 (2005) 1911–1919.
[24] J. Beck, S. Unterberger, Fuel 86 (2007) 632–640.
[25] N.-Y. Topsøe, T. Slabiak, B.S. Clausen, T.Z. Srnak, J.A. Dumesic, Journal of Catalysis 134 (1992) 742–746.
[26] J.R. Van Wazer, Phosphorus and Its Compounds, Interscience Publisher, New York, 1958.